

# Thermosensitive Micelles from PEG-Based Ether-anhydride Triblock Copolymers

Aijun Zhao · Shaobing Zhou · Qi Zhou · Tao Chen

Received: 20 January 2010 / Accepted: 8 April 2010 / Published online: 29 April 2010  
© Springer Science+Business Media, LLC 2010

## ABSTRACT

**Purpose** The thermosensitive micelles based on the poly (PEG:CPP:SA) terpolymer composed of poly(ethylene glycol) (PEG), 1,3-bis(carboxyphenoxy) propane (CPP) and sebacic acid (SA) were fabricated for application as a promising drug carrier.

**Methods** The terpolymer can self-assemble into micelles in water by a precipitation technology. The sol–gel transition behaviors were investigated by the tube-tilting method and dynamic rheology. The drug release behaviors were investigated in phosphate-buffered solution (PBS) at 25, 37 and 45°C, respectively, and the tumor cell growth inhibition assays were also evaluated.

**Results** The diameters of these micelles increased as the environmental temperature, and the length of CPP and SA chains increased. The micelles with a low concentration underwent sol-to-nanogel transition as temperature increased from the room temperature to the body temperature, while the polymer solutions with a high concentration underwent sol-to-gel transition as the temperature increased from 20 to 70°C. *In vitro* release profiles consisted of a burst release followed a sustained release. The cytotoxicity results showed that the terpolymer micelles were biocompatible, and the encapsulated doxorubicin. HCl maintained its potent anti-tumor effect.

**Conclusion** These micelles may bring the ether-anhydride family of polymers great potential as a novel carrier in nanomedicine.

**KEY WORDS** biodegradable · ether-anhydride · polymeric micelles · self-assemble · thermo-responsive

## INTRODUCTION

Polymeric micelles formed by self-assembly of amphiphilic block copolymers exerted many merits, such as nano-scale size, core-shell structure, relatively high stability due to low critical micellisation concentration (CMC), and prolonged circulation owing to their high water solubility (1–3). Their unique core-shell architecture consists of hydrophobic segments as internal core and hydrophilic segments as surrounding corona in aqueous medium, and poorly water-soluble drugs can be solubilized within the hydrophobic core of the micelle. As a result, polymeric micelles can substantially improve the solubility and bioavailability of various hydrophobic drugs (4,5). Drugs to be delivered can be covalently attached prior to micellization or vesicle formation or entrapped into the micellar core or polymer—some by the use of various techniques like solution/precipitation, salting-out process, and solvent evaporation method (6,7).

In recent years, several amphiphilic block copolymers have been synthesized with a particular interest (4,8,9). The amphiphilic diblock copolymers have also been widely studied mostly using aliphatic polyesters, such as poly( $\epsilon$ -caprolactone) (PCL), poly(D,L-lactide) (PLA), poly(glycolide) (PGA), and their copolymer poly(lactide-co-glycolide) (PLGA) as hydrophobic segments and polyether, such as PEG, as hydrophilic segments. The self-assemblies of these amphiphilic block copolymers have been shown to be of significant importance in many research fields (10–14), e.g. as building blocks for the fabrication of novel organic nanotubes, candidates for drug delivery and nano/micro-

A. Zhao · S. Zhou (✉) · Q. Zhou · T. Chen  
Key Laboratory of Advanced Technologies of Materials  
Ministry of Education, School of Materials Science and Engineering  
Southwest Jiaotong University  
Chengdu 610031, People's Republic of China  
e-mail: shaobingzhou@swjtu.cn

reactors for carrying on some reactions in aqueous solution (15). Furthermore, by use of stimuli-sensitive polymers (temperature, pH, etc.) as a part of the amphiphilic copolymers, it is possible to achieve a controlled release of encapsulated drugs from micelles in response to environmental changes (16–20).

There has been marked progress in the search for thermo-sensitive polymers during the last decade. Several thermo-responsive polymeric micelles have been extensively studied, such as poly(*N*-isopropylacrylamide) (PNIPAAm) (21,22), poly(ethylene oxide)-poly(propylene oxide)-poly(ethylene oxide) triblocks (PEO-PPO-PEO) (23–25), poly(ethylene glycol)-poly( $\epsilon$ -caprolactone) (PECL), chitosan glycerolphosphate, ethyl(hydroxyethyl) cellulose (EHEC) formulated with ionic surfactants (16,26–28) and poly(ethylene glycol)-poly(lactic acid)-poly(ethylene glycol) triblocks (PEG-PLA-PEG) (29). The thermo-sensitivity of these block copolymers micelles could be modulated by the alteration of the concentration of the aqueous solution, the composition of the copolymers, and so forth (30). Importantly, these block copolymer micelles consisting of PEG and biodegradable polyesters, such as PLA, PLGA and PCL, were found to be thermo-responsive and biodegradable, making them potential candidate materials for use in biomedical applications such as drug delivery, cell therapy and tissue engineering via *in situ* gel formation by simple injection (31).

A new family of high molecular-weight polymers designed for controlled drug delivery following inhalation or injection, poly(ether-anhydrides), have been successfully developed recently (32). These materials were used to produce drug-loaded microparticulates capable of injection via small needles or aerosolization as a dry powder. Amphiphilic triblock copolymers composed of hydrophobic sebacic acid (SA) end segments and hydrophilic interior blocks of PEG were synthesized via melt condensation by Zhang *et al.* (33), and the stable micelles could be formed from this polymer in an aqueous phase. PEG introduced into the polymer backbone significantly changed particles' hydrophilicity, surface roughness, surface charge and water content and could provide a steric barrier to reduce particles aggregation. Lee *et al.* (34) also designed PEG connected by SA segments of which the aqueous polymer solution is expected to undergo sol-to-gel transition as the temperature increases. These amphiphilic polymers consist of the flexible methylene units of SA and hydrophilic PEG. The hydrophilic/hydrophobic balance of the PEG-SA is a key factor in determining thermo-sensitive sol-gel transition at a desired temperature. The properties of the sol-to-gel transition can be altered by the PEG content of the copolymer backbone.

In this paper, we extended our investigation to the design and synthesis of amphiphilic PEG-based ether-anhydride

terpolymers via melt polycondensation. The terpolymers consisted of CPP, SA and PEG. Contrary to the PEG comprising the hydrophilic block, the CPP and SA chains were chosen as the hydrophobic blocks in the backbone of the terpolymers. Polyanhydrides comprised of CPP and SA are believed to predominantly undergo surface erosion, and the drug can be released by steady speed from the polymer matrix in drug delivery system. Hundreds of polyanhydrides have been synthesized in the recent decades, but only poly(sebacic anhydride) and its derivations have been applied in controlled drug delivery system. Secondly, the degradation rate of SA segments is much faster than that of CPP segments, owing to more hydrophilicity for SA than CPP. Finally, the hydrophilic/hydrophobic balance of the poly(PEG:CPP:SA) is a key factor in determining thermo-sensitive sol-gel transition at a desired temperature. In view of these factors, both SA and CPP were used as hydrophobic blocks in order to adjust the degradation rate and the hydrophilic/hydrophobic balance of the terpolymers. Incorporation of PEG could not only increase the hydrophilicity but also minimize protein adsorption (13). These amphiphilic terpolymers can self-assemble into polymeric micelles in the solvents that are selective for only one of the blocks. To the best of our knowledge, the thermo-sensitive micelles based on these terpolymers were prepared by the precipitation technology for the first time. Nanoprecipitation offers the advantages of simple and gentle formulation under ambient conditions without the use of chemical additives or harsh formulation processes (15). The properties of micelles were measured by atomic force microscopy (AFM), transmission electron microscopy (TEM) and dynamic light scattering measurements (DLS). The morphology and average size were also described by altering the hydrophilic/hydrophobic ratio, concentration of polymer in solution and temperature. The sol-to-gel transition in the terpolymer aqueous solution with a high concentration was further investigated with the temperature increasing in view of its potential application as *in situ* injected gel. Later, the cytotoxicity of the polymeric micelle was evaluated based on an osteoblast proliferation study. Finally, these polymeric micelles-encapsulated doxorubicin hydrochloride (DOX.HCl) were used to investigate their function of suppressing the growth of tumor cells with culturing with HepG2 tumor cells.

## MATERIALS AND METHODS

### Materials

All compounds and solvents used were obtained from Chengdu KeLong Chemical Reagent Company (Sichuan, Chengdu, China). These mainly include succinic anhydride, sebacic acid (SA), poly(ethylene glycol) (PEG,  $M_n =$

4,000 Da), 1,3-Dibromopropane, *p*-hydroxybenzoic acid. SA was recrystallized two times from ethanol. Acetic anhydride was refluxed over and distilled from magnesium. All other solvents were used as received without further purification. 1, 3-Bis-(carboxyphenoxy) propane (CPP) was synthesized according to the method described by previous literature (35). The cells were from the neonatal rat mandibular osteoblasts; HepG2 tumor cells were purchased from the American Type Culture Collection (ATCC; Rockville, MD, USA). Doxorubicin hydrochloride (DOX.HCl) was purchased from Zhejiang Hisun Pharmaceutical Co., Ltd. (China).

### Synthesis and Characterization of the PEG-Based Ether-anhydride Terpolymers

The PEG-based ether-anhydride terpolymers were successfully synthesized via melt-condensation polymerization without catalyst, as in the previous literature (32). Infrared spectra were obtained using a Nicolet 5700 spectrometer. The samples were pressed into KBr pellets for analysis. <sup>1</sup>H-NMR spectra were obtained on a Bruker AM 300 apparatus using CDCl<sub>3</sub> as a solvent and TMS as an internal reference. Chemical shifts were expressed as parts per million, ppm (δ). Gel permeation chromatography (GPC) measurements were carried out with a Water 2695 separation module equipped with a Styragel HT4DMF column operated at 40°C and series 2414 refractive index detector. Waters millennium module software was used to calculate molecular weight on the basis of a universal calibration curve generated by narrow molecular weight distribution polystyrene standards.

<sup>1</sup>H-NMR(CDCl<sub>3</sub>): δ 6.97, 7.99(d, ArH), 4.25(s, CH<sub>2</sub>), 3.66(s, OCH<sub>2</sub>CH<sub>2</sub>O), 2.44(t, CH<sub>2</sub>), 2.33(m, CH<sub>2</sub>), 1.65(m, CH<sub>2</sub>), 1.32(s, CH<sub>2</sub>). IR(KBr, cm<sup>-1</sup>): ~1,812–1,738, ~1,720 (C=O anhydride), 1,124 (CH<sub>2</sub>OCH<sub>2</sub>).

### Micelle Preparation and Characterization

The blank polymeric micelles were prepared using a precipitation method. In brief, preweighed terpolymer was first dissolved in 5 mL THF in a 50 mL flask, and then the solution of the copolymer was added dropwise into 10 mL deionized water using a disposable syringe (21 gauge) under high-speed stirring. Finally, the mixed solution was devolved to a beaker and slowly stirred for 4 h at room temperature to facilitate the removal of the THF. Once the THF had been removed completely, the solution was diluted with deionized water to the desired concentration.

The DOX.HCl-loaded polymeric micelles were fabricated as follows. In brief, poly(PEG:CPP:SA) (20:20:60) terpolymers (20.0 mg) in THF (4.5 mL) and DOX.HCl (1.0 mg) in double distilled water (0.5 mL) were mixed under high-speed stirring.

This solution was added dropwise into 10 mL of deionized water and stirred for 4 h. After the THF was removed by the evaporation, the transparent dark red solution was centrifuged and rinsed using deionized water 3 times to remove the excess DOX.HCl. The concentrated solution was lyophilized to leave a dark red powder of DOX.HCl-loaded micelles. Drug-loading efficiency and drug-loading content were determined from the ratio of the weight of the DOX in micelles to that of the micelles by the UV-Vis spectrophotometer.

Transmission electron microscopy observation was performed with a HITACHI H-700H (TEM, Japan) at the acceleration voltage of 150 kV. TEM sample was prepared by dipping a copper grid with Formvar film into the freshly prepared micelles solution. A few minutes after the deposition, the aqueous solution was blotted away with a strip of filter paper and stained with phosphotungstic acid aqueous solution, then dried in air.

The mean size and size distribution were determined by dynamic light scattering (DLS) using a ZETA-SIZER, MALVERN Nano-ZS90 (Malvern Instruments Ltd., Malvern, U.K.). Each measurement was also repeated 3 times and an average value reported.

The properties of the micelles were by Tapping-mode atomic force microscopy (AFM) measurements (CSPM5000, Beijing, China). The AFM sample was prepared by casting a dilute micelles solution on a slid silicon piece, which was then dried under vacuum.

A change in the fluorescence excitation spectra of pyrene in the presence of varied concentrations of block copolymers was used to measure the CMC. Pyrene was dissolved in acetone and added to 5 mL volumetric flasks to provide a concentration of  $6 \times 10^{-7}$  M in the final solutions. Acetone was then evaporated and replaced with aqueous polymeric micelle solutions with concentrations ranging from 0.05 to 500 μg/mL. The excitation spectrum of pyrene for each sample was obtained at room temperature using a Fluoromax spectrometer (F-7000, Hitach, Japan). The emission wavelength and excitation bandwidth were set at 390 and 5 nm, respectively. The intensity ratio of peaks at 339 nm to those at 333 nm was plotted against the logarithm of terpolymer concentration to measure CMC (36).

The polymeric micelle solutions were stored at a low temperature to equilibrate for 30 min before the ultraviolet (UV) measurements (UV-2550, Shimadu, Japan). The experimental temperature range was 25–50°C in increments of 2° C. At least 20 min was allowed for the temperature equilibration of the sample. The opaque temperature was determined as the onset point of the abrupt increase in the UV absorption, and the precipitate temperature was determined when the precipitate of the solution was formed. The LCST of the polymer solution was defined as the temperature

producing a half increase of the total increase in optical absorbance (25).

### Sol–Gel Transition

The sol (flow)–gel (no flow) transition behaviors of the terpolymers in aqueous solution were investigated by the tube tilting method, with a temperature increment of 2°C. Each sample with a given concentration was prepared by dissolving the polymer in ultrapure water in a 5 mL vial at room temperature for 2–3 h. The vial was immersed in a water bath at each temperature for 30 min to equilibrate. The sol–gel transition temperature was determined by tilting the vials to 90° for 10 min. If there was no flow in 10 min, it was regarded as a gel state.

The sol-to-gel transition behaviors of the polymer aqueous solution were further investigated by Bohlin Gemini 200 (Malvern Instruments Ltd., Malvern, U.K.). The polymer aqueous solution was placed between parallel plates with 25 mm diameter and 0.5 mm of a gap. The data were collected under a controlled stress (4.0 dyn/cm<sup>2</sup>) and a frequency of 1.0 rad/s. The heating rate was 1°C/min.

### In Vitro Drug Release Test

Pre-weighed DOX.HCl-loaded micelles were suspended in test tubes containing phosphate-buffered solution (PBS) at pH 7.4 at 25°C, 37°C and 45°C, respectively. The test tubes were kept in a thermo-stated incubator (Haerbin Dongming Medical Equipment Company) which was maintained at 107 cycles per minute. At predetermined intervals, 1.0 mL of supernatant was collected, and 1.0 mL of fresh PBS was added to the test tube. Concentration of drug released was determined by using an UV-visible spectrophotometer at absorbance of 232 nm.

### In Vitro Cytotoxicity Study

The cytotoxicity of the micelles was evaluated using an MTT assay (37). Osteoblasts from SD rat were cultured in Dulbecco's modified eagle's medium (DMEM) supplemented with 10% fetal bovine serum (FBS) at 37°C in a 5% CO<sub>2</sub> incubator. They were seeded in 24-well plates in 2.0 mL medium per well at a density of 10,000 cells/well for 6 h. The medium was then replaced with 2.0 mL of medium-containing micelles at the concentrations of 0.25 mg/mL, 0.5 mg/mL, 1.0 mg/mL and 2.0 mg/mL, respectively, and incubated for 24 h under 5% CO<sub>2</sub> at 37°C. After 24 h, the culture medium was removed from cell monolayers cultured in 96-well plates. Each well was reconstituted with 0.2 mL supplemented RPMI-1640 containing 1.0 mg/mL MTT and incubated the cultures for 2–4 h at 37°C. The supernatants were removed from the

wells, and then 0.2 mL dimethyl sulphoxide (DMSO) per well was added in isopropanol and mixed with the content of the wells thoroughly. Finally, the plates were read in an automated microplate spectrophotometer (ELX800 Biotek, USA) at 570 nm as reference. Every 24 h, the same tests were performed as mentioned above until 72 h.

The Hep G2 tumor cells were planted at a density of  $1 \times 10^4$  cells per well in 100  $\mu$ L of medium in 96-well plates and grown for 48 h. The cells were then exposed to a series of DOX.HCl-loaded polymeric micelles at different concentrations for 48 h, and DOX.HCl solution in DMSO at the same concentration was used as a control. Finally, viability of cells was measured using the MTT method. All data were expressed as the mean  $\pm$  S.D. The stained cells were observed under a fluorescence microscopy (DMR HCS, Leica, Germany).

## RESULTS AND DISCUSSION

### Characterization of the Terpolymers

The structure of poly(PEG:CPP:SA) triblock copolymer was confirmed by FT-IR, <sup>1</sup>H-NMR, and GPC. Poly(CPP:SA) copolymers have been investigated widely. Fig. 1(a) displays the typical FT-IR spectra of poly(CPP:SA) and poly(PEG:CPP:SA) terpolymers with weight ratios of PEG4000 at 20% and 40%. The absorption bands at 1,812 and 1,738 cm<sup>-1</sup> are the characteristic peaks of SA anhydride carbonyl, and the peaks at 1,812 and 1,720 cm<sup>-1</sup> are attributed to CPP anhydride carbonyl. The C–H stretching vibrations of long aliphatic alkyl and the PEG are distributed at 2,900 and 2,850 cm<sup>-1</sup>. With the amount of PEG in the terpolymers increasing, the intensity of peaks at 1,124 cm<sup>-1</sup> attributed to the characteristic C–O–C stretching vibration also increases. The absorption band at about 3,500 cm<sup>-1</sup> is assigned to terminal hydroxyl groups in the hydrolysate from which terpolymers have been sopped up. Simultaneously, the absorption band at 1,812 cm<sup>-1</sup> decreases when the content of SA reduced. These phenomena suggests that the poly(PEG:CPP:SA) terpolymers have been synthesized successfully.

<sup>1</sup>H-NMR spectrum is shown in Fig. 1(b) in order to further confirm the formation of these terpolymers. The well-resolved chemical shifts at  $\delta$ =1.32, 1.66, 2.26, and 2.44 ppm belong to the hydrogen atoms of individual functional groups on poly(sebacic anhydride). The chemical shifts at 1.66, 2.33, 4.25, 6.97, and 7.99 ppm ascribe to the protons of CPP. The sharp single peak at 3.66 ppm is attributed to the methylene protons of homosequences of the PEG units. The peak at 7.25 ppm corresponds to the solvent, deuterated chloroform. These results are consistent with the information obtained from FT-IR. The actual

weight percentages of PEG, CPP, and SA in the polymers were estimated from the integral height of hydrogen atoms in the  $^1\text{H-NMR}$  spectra. All the synthesized products have approximate segmental ratios of monomer units to the

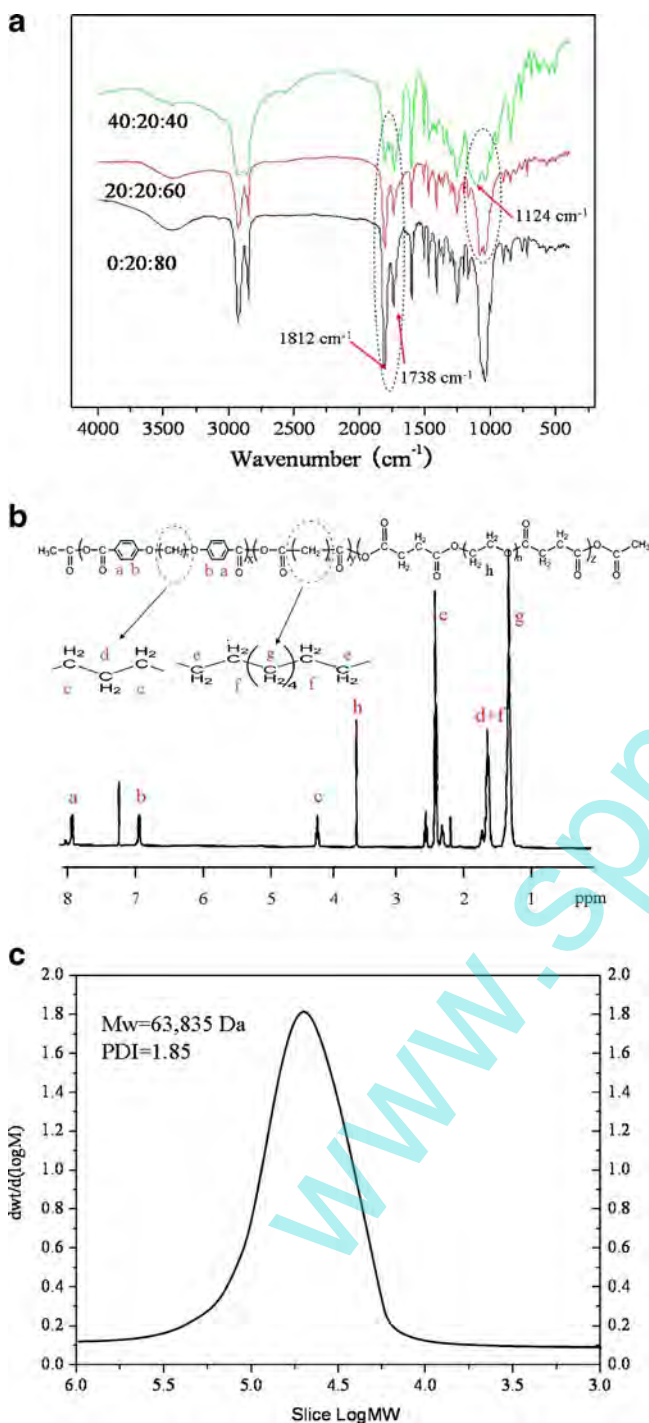


**Fig. 1** **a** FT-IR spectra of the poly(PEG:CPP:SA) terpolymers with weight ratios of 0:20:80, 20:20:60 and 40:20:40; **b**  $^1\text{H-NMR}$  spectra of poly(PEG:CPP:SA) (20:20:60) ( $^1\text{H-NMR}$  spectra were measured using  $\text{CDCl}_3$  as a solvent), **c** GPC curve of poly(PEG:CPP:SA) (20:20:60) terpolymers (average Mw and its distribution were determined by GPC operating with THF).

feeding composition, which are summarized in Table I. The yield of the copolymers ranged from 65.0% to 72.5%.

The terpolymers are also characterized by GPC to determine their Mw. Fig. 1(c) shows the GPC curve of poly(PEG:CPP:SA) (20:20:60) terpolymers. The terpolymer poly(PEG:CPP:SA) (20:20:60) containing roughly 20 wt% PEG, 20 wt% CPP and 60 wt% SA has a Mw of 63,835 Da, whereas poly(PEG:CPP:SA) (40:20:40) has a Mw of 41,123 Da, as summarized in Table I, probably because the introduction of PEG constrained the development of polymer chains following melt-polycondensation (38). As seen from the GPC curve, there was not bimodal distribution, which also indicated that the terpolymer was achieved. By altering the content of PEG in the terpolymers, their PDI ranged between 1.85 and 2.35. The polycondensation reaction usually gives rise to such a polydispersity. Thus, the terpolymers synthesized in this experiment could be processed into micelles using the precipitation method.

### Characterization of the Polymeric Micelles

Polymeric micelles have received much attention as a material for drug delivery systems, since the incorporation can be achieved without the active sites being destroyed by harsh reactions in conjugation step, and at the same time the self-assembly is eventually formed without a cross-linker (15). Typically, the ionic (or hydrophilic) head groups are exposed to the bulk aqueous solution, while the hydrophobic hydrocarbon tail groups form the interior of the micelle. Herein, the precipitation method was used for preparation of micelles without any surfactant. As most of the micelles cases, the main attractive driving force for the poly(PEG:CPP:SA) terpolymers micellization is hydrophobic interaction and entropy driven.

In order to determine the CMC of poly(PEG:CPP:SA) micelles, fluorescence measurements were carried out using pyrene as a fluorescent probe (36). Compared with the micelles with low molecular-weight surfactant, polymeric micelles are generally more stable, exhibiting a remarkably lower CMC (39). Typical CMC ranges are from  $10^{-4}$  to  $10^{-2}$  g/L for most of the amphiphilic polymers. As shown in Fig. 2a, the intersection point at  $C=0.00259$  g/L is estimated to be the CMC of the poly(PEG:CPP:SA) (20:20:60) terpolymer at  $25^\circ\text{C}$ . Fig. 2d summarizes the CMC values of the various compositions of poly(PEG:CPP:SA) terpolymers. These values are much lower than those of low molecular-weight surfactants, indicating that micelles formed from the terpolymers as drug carriers can keep stability without dissociation after dilution caused by intravenous injection. The hydrophilicity of poly(PEG:CPP:SA) terpolymers mainly depends on the PEG/(CPP and SA) ratio, which further influences the CMC value. As shown in Fig. 2d, the CMC values of poly(PEG:CPP:SA) (40:20:40)

**Table 1** Characterization of Poly(PEG:CPP:SA) Triblock Copolymers

PEG:CPP:SA In the feed <sup>a</sup> (wt%)	Yield (w%)	PEG:SA:CPP <sup>1</sup> H-NMR <sup>b</sup> (wt%)	M <sub>w</sub> <sup>c</sup> (Da)	PDI <sup>c</sup>
20 : 20 : 60	72.5	17.6:18.9:63.5	63,835	1.85
30 : 20 : 50	68.9	26.7:18.7:54.6	50,080	2.16
40 : 20 : 40	65.0	36.1:19.5:44.4	41,123	2.35

<sup>a</sup> Poly(ether-anhydrides) were synthesized by melting polymerization

<sup>b</sup> Estimated from the integral height of hydrogen atoms in the <sup>1</sup>H-NMR spectra

<sup>c</sup> Obtained by GPC

terpolymers are higher than those of poly(PEG:CPP:SA) (20:20:60). Hydrophobic molecular chains of poly(PEG:CPP:SA)(20:20:60) terpolymers are much longer, and, consequently, they can self-assemble more easily to form micelles, leading

to lower CMC values. The lower CMC value indicates a strong tendency toward formation of aggregates (40).

DLS was employed to evaluate the average size and size distribution of the obtained micelles. Fig. 3 displays that the diameter of the poly(PEG:CPP:SA) terpolymers micelles is typically in the range of 80–200 nm. According to a previous report (41), the polymeric micelles with a size of less than 200 nm would reduce non-selective reticulo-endothelial system (RES) scavenging and show enhanced permeability and retention (EPR) effects at solid tumor sites for passive targeting. As shown in Fig. 3, the micelles with low polydispersity were formed from these terpolymers in an aqueous phase. The diameter of the micelles decreases with the increasing of the PEG content. The main reason is that the hydrophobic segments as internal core are smaller and the radius of curvature is increased when the

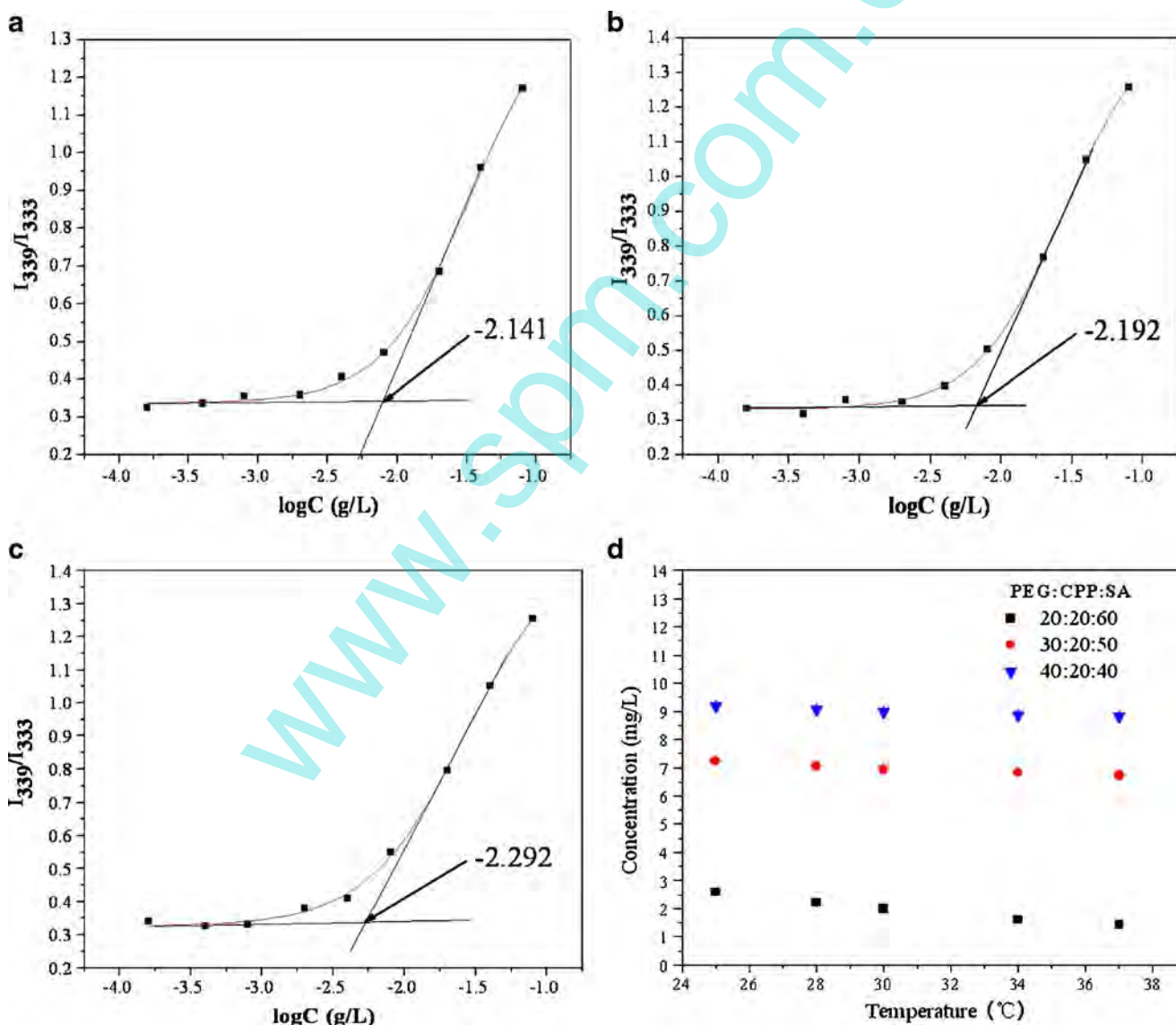


**Fig. 2** CMC of the poly(PEG:CPP:SA) (20:20:60) terpolymers at 25°C (a), 30°C (b) and 37°C (c) and CMC dependence on the structure of poly(PEG:CPP:SA) terpolymers and their corresponding aqueous solutions at different temperatures (d).

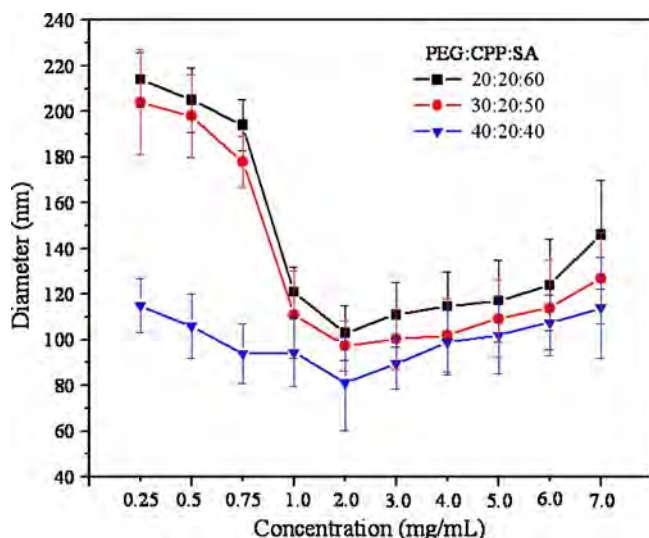


**Fig. 3** Average size of the poly(PEG:CPP:SA) terpolymers micelles in their aqueous solutions at different concentrations.

PEG amounts increase. The hydrophilic segments can form the outer shell to the micelle surface. The concentration of polymer aqueous solution should also have much influence on the size and its distribution of micelles. The micellization was a self-assembly due to the amphiphilic structure of poly(PEG:CPP:SA) terpolymer. Before the micelles are formed, the

number of the unimer increases with the increase of the polymer concentration when the polymer concentration is under the CMC, and thus the area occupied by each unimer becomes smaller, leading to increase in crowding of the tethered unimers. As the polymer concentration in aqueous solution exceeds the CMC, in order to reduce the crowding of the unimers and the repulsive force of the aggregations, the smaller micelles were formed during the self-assembly process. However, the number of the aggregates increased with the concentration increasing as the polymer concentration was beyond 2.0 mg/mL, which led to the micelle size increasing slightly.

The structure of the micelles was observed by TEM and AFM. Importantly, the morphology of the nanoscopic dimension has been shown to influence their performance in applications as nanocarriers (42). AFM technique as an effective method has been widely applied to obtain surface morphological information of micelles (43). Compared with TEM and DLS size, the AFM size may be slightly decreased because of the collapse of micelle during drying process. Herein, Fig. 4a1, b1 and c1 show the AFM images of the micelles of the poly(PEG:CPP:SA) terpolymers with different PEG content. We can find that all these micelles take on a spherical shape, which is in good agreement with the result of TEM. Furthermore, the poly(PEG:CPP:SA) (20:20:60) terpolymer micelles (2.0 mg/mL) with diameters

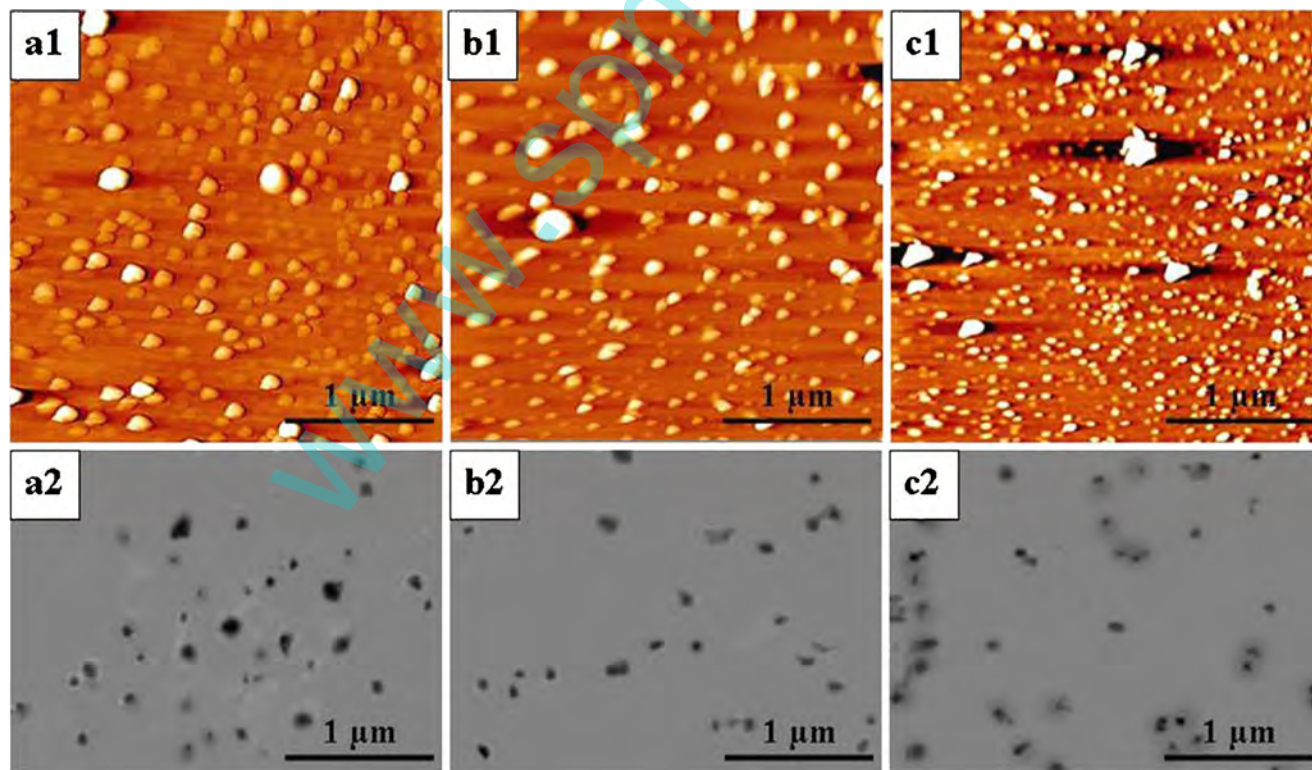


**Fig. 4** AFM (a1, b1, c1) and TEM (a2, b2, c2) image of the poly(PEG:CPP:SA) micelles (2.0 mg/mL) with PEG ratio of 20%, 30% and 40%, respectively.

typically in the range of 100–200 nm are observed in Fig. 4a1 and a2. Fig. 4c1 displays that the diameter of the poly(PEG:CPP:SA) (40:20:40) terpolymer micelles is smaller, which is consistent with the Z-average diameter of about 80 nm. This mainly resulted from the highest hydrophilicity due to the highest PEG ratio among these poly(PEG:CPP:SA) terpolymers.

### Aqueous Phase Behavior

Recently, developing thermo-responsive polymeric micelles as intelligent drug carriers that would react by a sharp change of properties in response to a small change of temperature has attracted much attention (44). Of utmost important is that we find that the synthesized terpolymers are also thermo-responsive. Temperature-related stability of micellar solutions was also investigated to better understand the micellization behaviors of the terpolymers under physiological temperatures. The CMC values of the terpolymers at 37°C are slightly lower than those at 25°C (Fig. 2d). This could be attributed to an increase in hydrophobicity or loss of polarity of PEG at elevated temperatures, thus leading to dehydration of PEG chains and a subsequent decrease in the CMC (39). Furthermore, the CMC values display a downtrend profile, with the temperature increasing as shown in Fig. 2d. However, the CMC of the terpolymer with the higher PEG ratio was changed more slightly with varied temperatures. This result suggested that the poly(PEG:CPP:SA) (40:20:40) micelles have better stability due to their higher hydrophilicity.

The solution behaviors of the thermo-responsive terpolymers were investigated by an optical method. Compared with the poly(PEG:CPP:SA) (30:20:50) and the poly(PEG:CPP:SA) (40:20:40) micelles, the poly(PEG:CPP:SA) (20:20:60) micelles have a more obvious thermo-responsive transition. To determine whether the poly(PEG:CPP:SA) (20:20:60) micelles (4.0 mg/mL) exhibit a thermal response, we first observed macroscopically that the solution of the polymeric micelles is almost transparent at room temperature and becomes opaque with the increases of the temperature and then precipitates (Fig. 5). Later, the optical absorbance of polymeric micelles in distilled water was measured as a function of temperature. The Z-average diameter of the poly(PEG:CPP:SA) (20:20:60) micelles in water at different temperatures was also measured by DLS as shown in Fig. 5. With the increase of the temperature, the hydrophobicity of the polymer was also improved, resulting in the micelles congregating and further leading to the increasing of the diameter of micelles. From Fig. 5, the break point of the absorbance could be obtained, and thus the opaque temperature and the precipitate temperature of the micelles solution were also achieved. For the poly(PEG:CPP:SA) (20:20:60) micelles solution

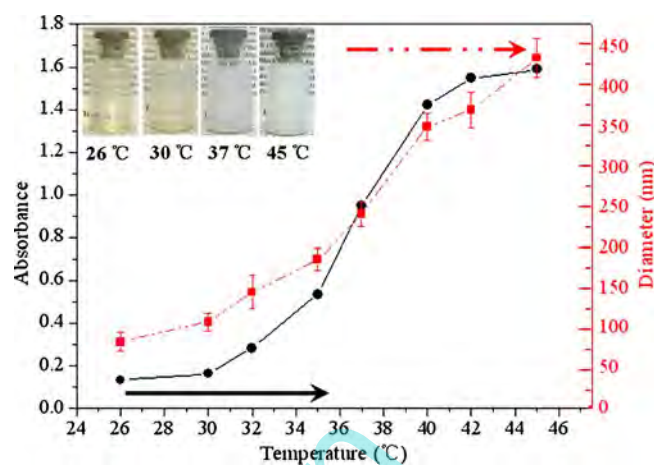


**Fig. 5** Absorbance and diameter changes of poly(PEG:CPP:SA) (20:20:60) aqueous solution (4.0 mg/mL) as a function of temperature, respectively. Insets are optical images of transparency of the micelle solutions in vials changed with altering temperature.

(4.0 mg/mL), the opaque temperature, lower critical solution temperature (LCST) and precipitate temperature are about 33.5°C, 36.5°C and 40.5°C, respectively. For the poly(PEG:CPP:SA) (30:20:50) micelles solution (4.0 mg/mL), these temperatures are changed to 37.5°C, 41.5°C and 44°C. However, there is no obvious change in the absorbance for the poly(PEG:CPP:SA) (40:20:40) micelles solution due to its strong hydrophilicity. Therefore, the followed investigation was mostly focused on poly(PEG:CPP:SA) (20:20:60) copolymer.

In order to obtain additional information concerning the temperature-responsive behavior, the micelle size and its distribution for the terpolymer micelles were measured by DLS at various temperatures. Fig. 6a shows the changes of the size and size distribution of poly(PEG:CPP:SA) (20:20:60) terpolymers micelles with the concentration of 1.0 mg/mL in an aqueous solution as a function of temperature. The mean diameter increases gradually, and the size distribution becomes more capacious at elevated temperatures. The polydispersity index (PDI) was increased from 0.235 at 25°C to 0.578 at 55°C. The trends of change in the size and its distribution for poly(PEG:CPP:SA) (30:20:50) and poly(PEG:CPP:SA) (40:20:40) terpolymers micelles were almost similar with the result. However, the poly(PEG:CPP:SA) (40:20:40) micelles have more stability, which is attributed to their higher hydrophilicity. Size of poly(PEG:CPP:SA) (20:20:60) micelles in the aqueous solutions at the different concentrations was also studied as displayed in Fig. 6b. An increase of the temperature results in an increase of the Z-average diameter of the micelles because of the micelles aggregation. Fig. 6c exhibits the diameter changes of the three types of copolymer aqueous solution (1.0 mg/mL) as a function of temperature. The diameters increased from about 90 to 220 nm for poly(PEG:CPP:SA) (40:20:40) terpolymers micelles and increased



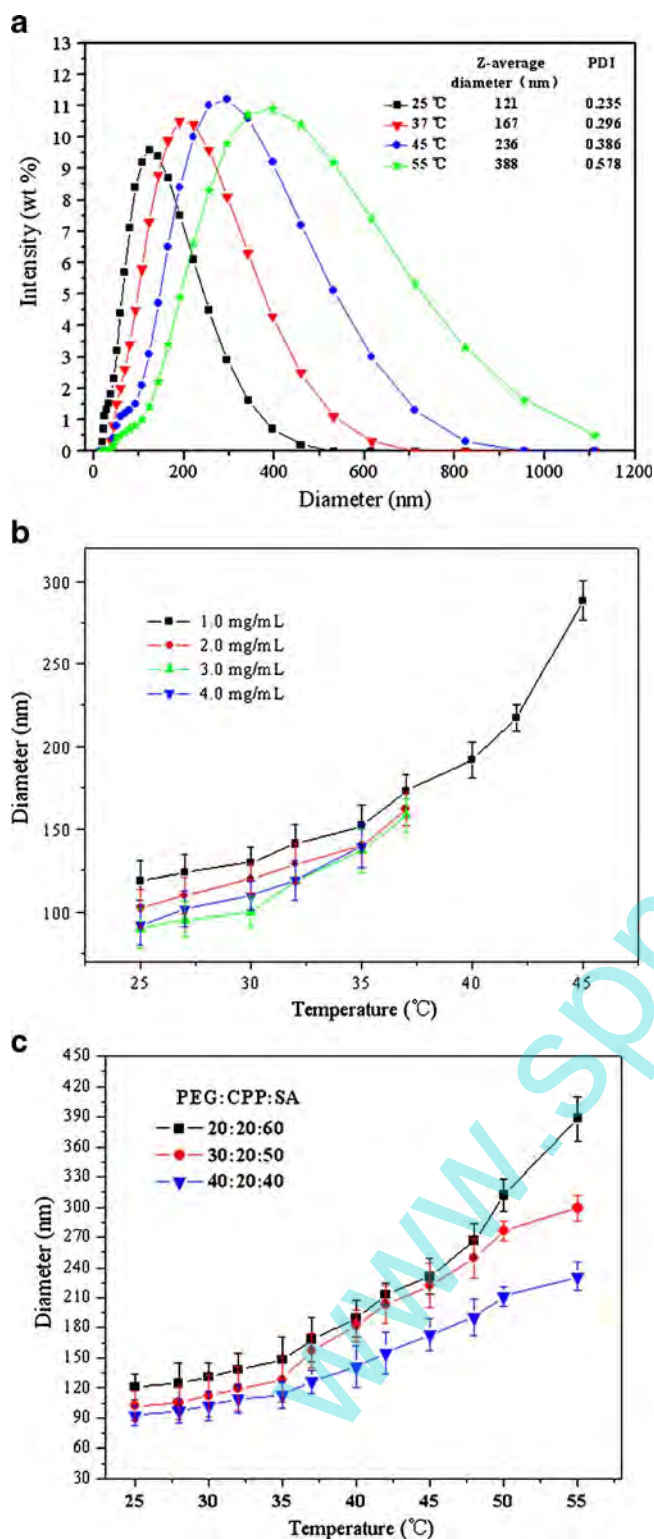


**Fig. 6** Size distribution of poly(PEG:CPP:SA) (20:20:60) micelles (1.0 mg/mL) (a), diameter changes of poly(PEG:CPP:SA) (20:20:60) solution with different concentrations (b) and of poly(PEG:CPP:SA) aqueous solution (1.0 mg/mL) comprised of different ratios of PEG, CPP and SA as a function of temperature (c).

from about 120 to 400 nm for poly(PEG:CPP:SA) (20:20:60) terpolymers micelles as the temperature was raised from 25°C to 55°C. Therefore, the terpolymers could self-assemble into stable micelles due to high hydrophilic-to-hydrophobic balance in an aqueous solution below the opaque temperature. In other words, the hydrophilicity of the polymeric micelles above the precipitate temperature seems not enough to form stable micelles, which means that the hydrophilic-to-hydrophobic balance of the thermo-responsive terpolymers is a critical factor to form stable micelles (45).

The typical thermo-responsive micelles transition of the poly(PEG:CPP:SA) micelles solutions was summarized in Fig. 7. These polymeric micelle solutions showed a transparency-turbidity-precipitate transition in response to the elevated temperature from 32 to 70°C. The transition temperature was found to be a function of both terpolymer concentration and structural composition. As shown in Fig. 7, an increase in the terpolymer concentration resulted in a decrease both in the opaque temperature and in the precipitate temperature. Besides the influence of copolymer concentration, structural composition of the terpolymers also exhibited an obvious effect on the thermo-responsive transition. When an increase in the PEG content in terpolymer backbone from 20% to 30% occurred, both the opaque temperature and the precipitate temperature transitions dramatically shifted to higher temperature. Furthermore, the terpolymers with a concentration in the range of 0.5–8.0 mg/mL existed as clear solutions at room temperature (25°C) and turned into an opaque solution (nanogel) at body temperature (37°C). Compared with the polymeric micelles, the nanogel has a better stability upon dilution, and a prolonged drug release from the nanogel could be achieved owing to the gradual degradation of the polymer matrix. The stability of these nanogels upon dilution was also studied; however, the obvious change of these nanogels upon dilution after several days was not observed. Thus, this physicochemical property makes these terpolymers more suitable for drug delivery applications (46).

A morphological transition at increasing temperature was further investigated, as shown in Fig. 8(1). The thermo-responsive transition of poly(PEG:CPP:SA) (20:20:60) micelles is more obvious and the micro-sized granules are obtained at 45°C (Fig. 8(1)c). Such a temperature-dependent morphological transition was coincident with the thermo-sensitive phase transition as previously studied (47). When the temperature was below the opaque temperature, the polymer micelles randomly suspended in aqueous solution. During the thermo-sensitive transition, the hydrophilic chains of the micelles shrunk at the initial stage of heating due to the dehydration, and then these micelles were joined together

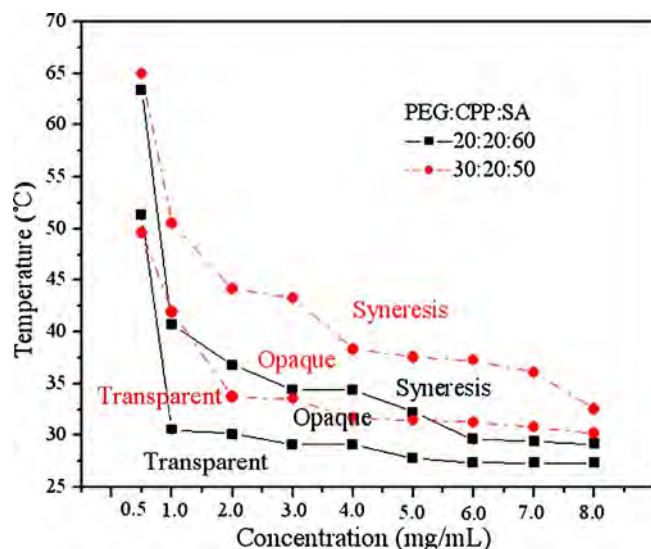
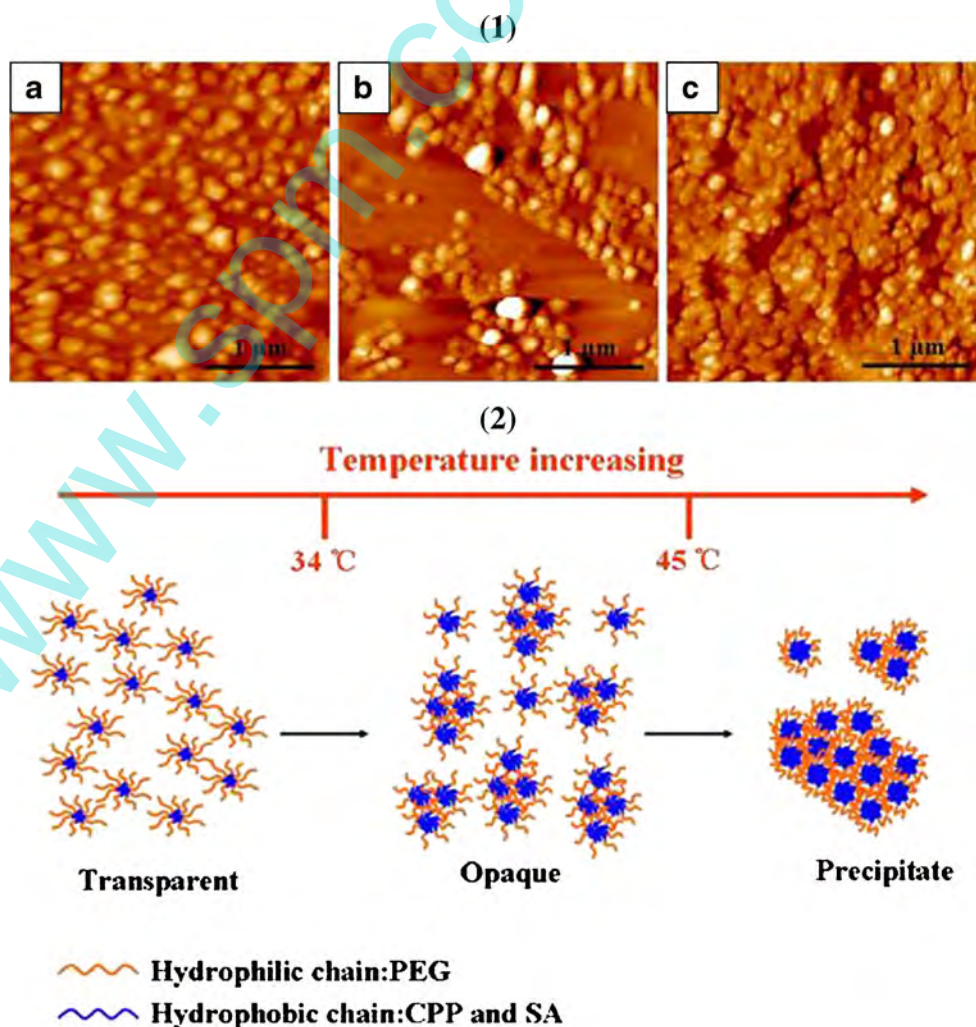


**Fig. 7** The effects of temperature and concentration on aqueous phase behavior of the poly(PEG:CPP:SA) micelles solutions.

**Fig. 8** **1** AFM image of the poly(PEG:CPP:SA) (20:20:60) micelles (4.0 mg/mL) at 25°C (a), 37°C (b) and 45°C (c); **2** Schematic illustration of the formation and behavior of the morphological transition of the polymeric micelles self-assembled as a function of temperature.



to form the larger aggregates because of the increase of intermicellar hydrophobic interaction (47). An increase of temperature leads to the increase in the average aggregation number. The micelle dehydration and aggregation will certainly increase the solution turbidity due to the scattering, the size of the diameter obtained by DLS and the morphological transition controlled by the temperature (48). Considering these results, it can be proposed that the individual primary micelles tend to combine together (intermicellar aggregation) with increasing solution temperature.

As shown in Fig. 8(2), the morphological transition of the polymeric micelles also results from the self-assembly of the poly(PEG:CPP:SA) terpolymers as a function of the temperature. The polymeric micelles are formed with the hydrated outer shell and the hydrophobic inner core as the temperature is below the opaque temperature. When the temperature exceeds the opaque temperature, the outer shell shrinks and becomes hydrophobic. Intermicellar aggregation may be formed on the basis

of both a micelle concentration and the strength of the shrunken outer shell layer's hydrophobic interactions. Above the precipitate temperature, the solution of the polymeric micelles seems not hydrophilic enough to make stable micelles; precipitates must occur when the micellar structure is broken because of the overhydrophobicity of the terpolymers (49). More importantly, the lower thermodynamic stability of micelle shells is one of the reasons for a relatively lower temperature of the sol-nanogel transition. Thus, the temperature-responsive phase transition of the amphiphilic terpolymers could demonstrate a strong correlation with aggregation (micelle formation) ability and intermicellar aggregation in an aqueous solution.

### Optical Sol-Gel Transition

*In situ* gel-forming polymers have recently drawn attention as materials for minimally invasive therapy (50). In particular, thermo-gelling biodegradable polymers with a sol-gel transition point between the room temperature and the body temperature are expected to be useful for injectable polymer systems in biomedical applications. The sol-gel transition behavior of the poly(PEG:CPP:SA) terpolymers in aqueous solution was investigated by the tube-tilting method. After the samples were stabilized for 30 min at measuring temperature, the sol-gel transition was determined by tilting the vials to 90° for 10 min. Fig. 9a shows the sol-gel transition behavior of poly(PEG:CPP:SA) (20:20:60) terpolymers and poly(PEG:CPP:SA) (30:20:50) terpolymers in aqueous solution. A critical gelation temperature was determined through both the culmination of the storage modulus and the tube-tilting method (51). The phase diagrams exhibited critical gel concentration (CGC) and two critical gelation temperature (CGT) curves (a lower transition temperature curve from sol to gel and an upper transition temperature curve from gel to precipitation). Both the poly(PEG:CPP:SA) (20:20:60) and the poly(PEG:CPP:SA) (30:20:50) terpolymers have the low CGC (4 wt%). As SA segments were increased from 50 wt% to 60 wt% in the poly(PEG:CPP:SA) terpolymers, the temperature of the critical point moved from 50 to 34°C, and the hydrophobic chains got longer, micelles were generally formed with a less number of associated chains. Thus, the more intra- or intermicelle phase mixing between micelles would produce more grouped micelles, inducing sol-to-gel phase transition at lower temperatures (51). As the terpolymer concentration increased, the sol-gel temperature decreased and the gel-precipitation temperature increased, probably due to an increase in the availability of physical cross-linking points (52). The photographs in Fig. 9a also show the sol-gel surface transition of the poly(PEG:CPP:SA) terpolymers.

Below the sol-to-gel transition temperature, the solution is liquid, while the solution becomes stagnant above the CGT, and the precipitation is observed above the gel-to-precipitation temperature. In general, in order to attain

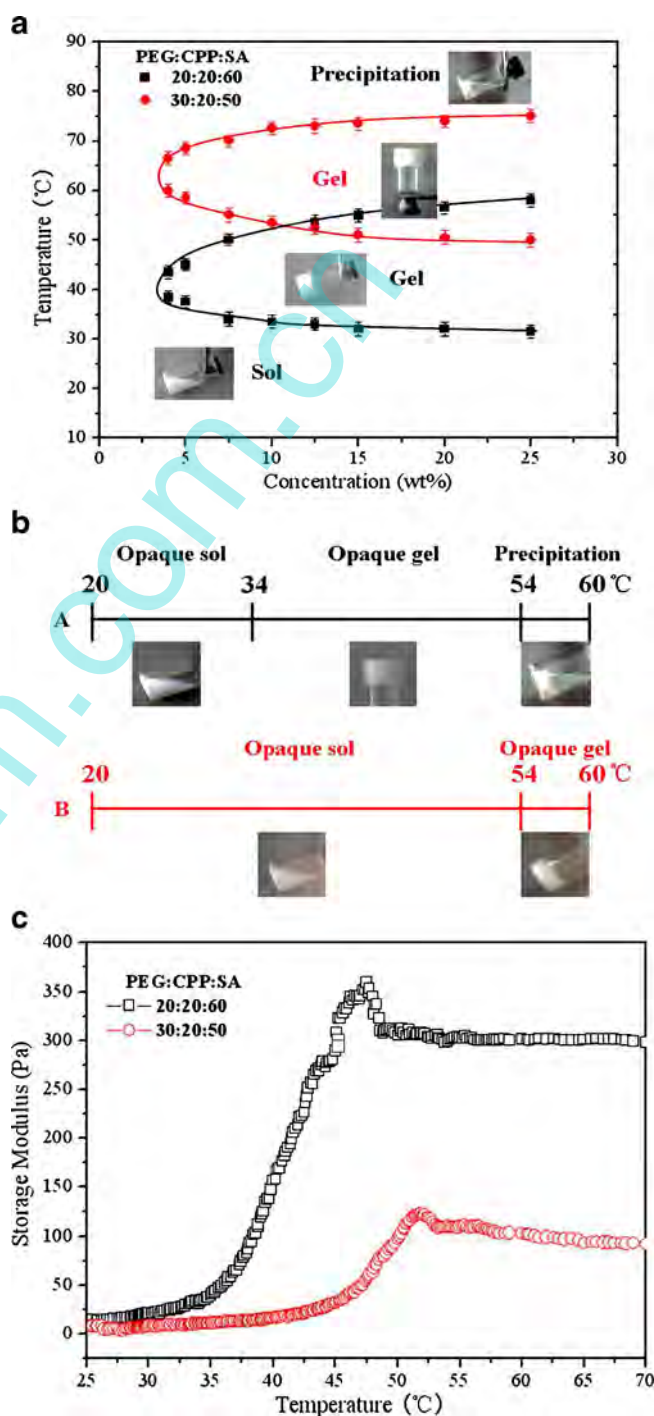


**Fig. 9** **a** Effect of the relative hydrophobicity of CPP and SA chains on the sol-gel transition of the copolymer aqueous solutions, **b** Physical gelation behavior of the thermosensitive poly(PEG:CPP:SA) terpolymers (10 wt%) in water. A: poly(PEG:CPP:SA) (20:20:60), B: poly(PEG:CPP:SA) (30:20:50), **c** Changes in storage modulus of the poly(PEG:CPP:SA) aqueous solutions (10 wt%) as a function of temperature.

relatively stable gels, most polymer concentrations are usually around 10 wt% (53).

Fig. 9b displays the physical gelation behavior of the poly(PEG:CPP:SA) (20:20:60) (10 wt%) and the poly(PEG:CPP:SA) (30:20:50) terpolymers (10 wt%). On heating, a 10 wt% aqueous solution of the poly(PEG:CPP:SA) (20:20:60) terpolymers underwent sensitive physical gelation leading to opaque gel. Above 34°C and below 54°C, the sol–gel transition of the poly(PEG:CPP:SA) (20:20:60) terpolymers (10 wt%) occurred. In contrast, the poly(PEG:CPP:SA) (30:20:50) terpolymer (10 wt%) did not display an apparent increase in viscosity at the same temperature range. Above 54°C, the precipitation of the poly(PEG:CPP:SA) (20:20:60) terpolymer (10 wt%) was formed. The sol–gel transition of the poly(PEG:CPP:SA)(30:20:50) terpolymer (10 wt%) occurred at about 54°C. The physical gelation occurrence was dependent to a considerable extent on the timing needed to form micelles and their stability (51). In this study, the sol–gel transition was obtained through 30 min. In the sol phase of the poly(PEG:CPP:SA) terpolymers, the opaque temperature depends on the hydrophobic chain ratio of polymer backbone, that is, the polymer chains responded gradually to temperature around the sol-to-gel temperature.

The sol-to-gel transition accompanied an abrupt change in the modulus. The aqueous solution of the poly(PEG:CPP:SA) (20:20:60) (10 wt%) underwent a sol-to-gel transition at 34°C as the temperature increased, which accompanied a 10-multiple increase in the storage modulus ( $G'$ ) at the transition temperature and accompanied a 100-multiple increase in the storage modulus ( $G'$ ) at 47°C (Fig. 9c). It implied that a flexible and soft gel was formed at 34°C (the temperature of the sol–gel transition) and then the gel became rigid as the temperature increased. When the hydrophilic block (PEG) increased at the composition of the poly(PEG:CPP:SA) (30:20:50) (10 wt%), the sol-to-gel transition temperature increased, and the storage modulus of the gel decreased. Such trends suggest that the characters of the thermal gelation behavior should be mainly driven by the amphiphilic structure of the poly(PEG:CPP:SA) terpolymers. When the temperature decreased, there was not any hysteresis. Both the gel and the opaque solution of the poly(PEG:CPP:SA) terpolymer micelles are especially stable and almost irreversible as the temperature reversing. We did not observe the obvious changes of the opaque solution and the gel in 10 days and even 2 months.

To the best of our knowledge, there have been no reports concerning the temperature-responsive transition of amphiphilic ether-anhydride terpolymers in which the backbones are composed of CPP, SA and PEG, since such longer hydrophobic segments generally lead to insolubility in aqueous media. The sol–gel transition behavior of the poly(PEG:CPP:SA) terpolymers in aqueous solution was

slightly different from the reverse thermo-responsive phenomenon of several reverse thermal gelation (RTG)-displaying polymers. Both the gel and the opaque solution of the poly(PEG:CPP:SA) terpolymer micelles are especially stable and almost irreversible as the temperature reversing. The gel of the poly(PEG:CPP:SA) terpolymers in aqueous solution is holding for 30 days so much as more days at room temperature. Thus, we consider that the sol–gel transition behavior of the poly(PEG:CPP:SA) terpolymers has poor reversibility. The reason may be that the re-assembly of the micelle should be restrained due to the long hydrophobic chains of CPP and SA in the terpolymers backbone as a function of temperature. Irreversible self-assembly processes that can often occur by sudden strong imposition of intermolecular or colloidal forces (e.g., by force shock) or by just pure random chance also can be problematic for the operation of nanodevices (53). On the other hand, this sol–gel transition is irreversible, which should be due to the stronger hydrophobic structure of the random backbone of the special terpolymers. For example, hydrophobic A-blocks consisting of PLA will associate, leading to a core-corona structure with dangling PEG chains in the case of BAB polymers and PEG loops in the case of ABA polymers. Gelation of the triblock copolymers is the result of dense micelle packing and phase mixing of the corona (PEG) with the core leading to chain entanglement in the ABA type or micellar bridging in the BAB type. The latter mechanism could lead to irreversible aggregation (52). The reason for poor reversibility of these terpolymer micelles will require further investigation. However, temperature ranges at which synthesized polymers showed sol-to-gel transition (lower transition) and gel-to-precipitation transition (upper transition) in the poly(PEG:CPP:SA) terpolymers solution indicate the possibility of the terpolymers as an injectable drug delivery carrier. As new thermosensitive polymer that are soluble at lower temperatures and become insoluble at higher temperatures in aqueous media, they must receive much attention, not only because of theoretical interest but also because of applications as drug reservoirs.

### Cell Cytotoxicity

One of the major requirements for terpolymer application in medicine should be non-toxicity. Although the poly(CPP:SA) is generally considered a biodegradable and safe polymer, the cytotoxicity of the poly(PEG:CPP:SA) (20:20:60) terpolymer micelles are performed by quantitative evaluation of cell viability using osteoblast cells. According to the MTT assay results (Fig. 10a), we can see that the samples of the terpolymers (2.0 mg/mL) performed a degree of cytotoxicity to reduce the cell viability compared to the control group. The cell viability expressed

in this study is relative to those at each concentration of the micelles. The change at the concentration from 2.0 to 0.25 mg/mL may influence cell viability, noting that the moderate concentration is a favorable environment for osteoblasts. This study underlined a fact that the terpolymers possess some cytotoxicity as the concentration is above 1.0 mg/mL, but the terpolymer micelles (0.25 mg/mL) can be made low toxic. Thus, the poly(PEG:CPP:SA) (20:20:60) terpolymer micelles can be suitable for various biomedical applications.

The cytotoxicity of the poly(PEG:CPP:SA) (20:20:60) terpolymer micelles with different concentrations were also evaluated by microscopically examining the osteoblast cells (Fig. 10(b)). The microscopic results were consistent with those obtained from the MTT assay. From these images, we can see that the morphology and the numbers of the sample with 0.25 mg/mL for the terpolymer micelles are similar with the control group, suggesting that the sample has good biocompatibility. In contrast, the cells became rounded and nonadherent as the concentration increased.

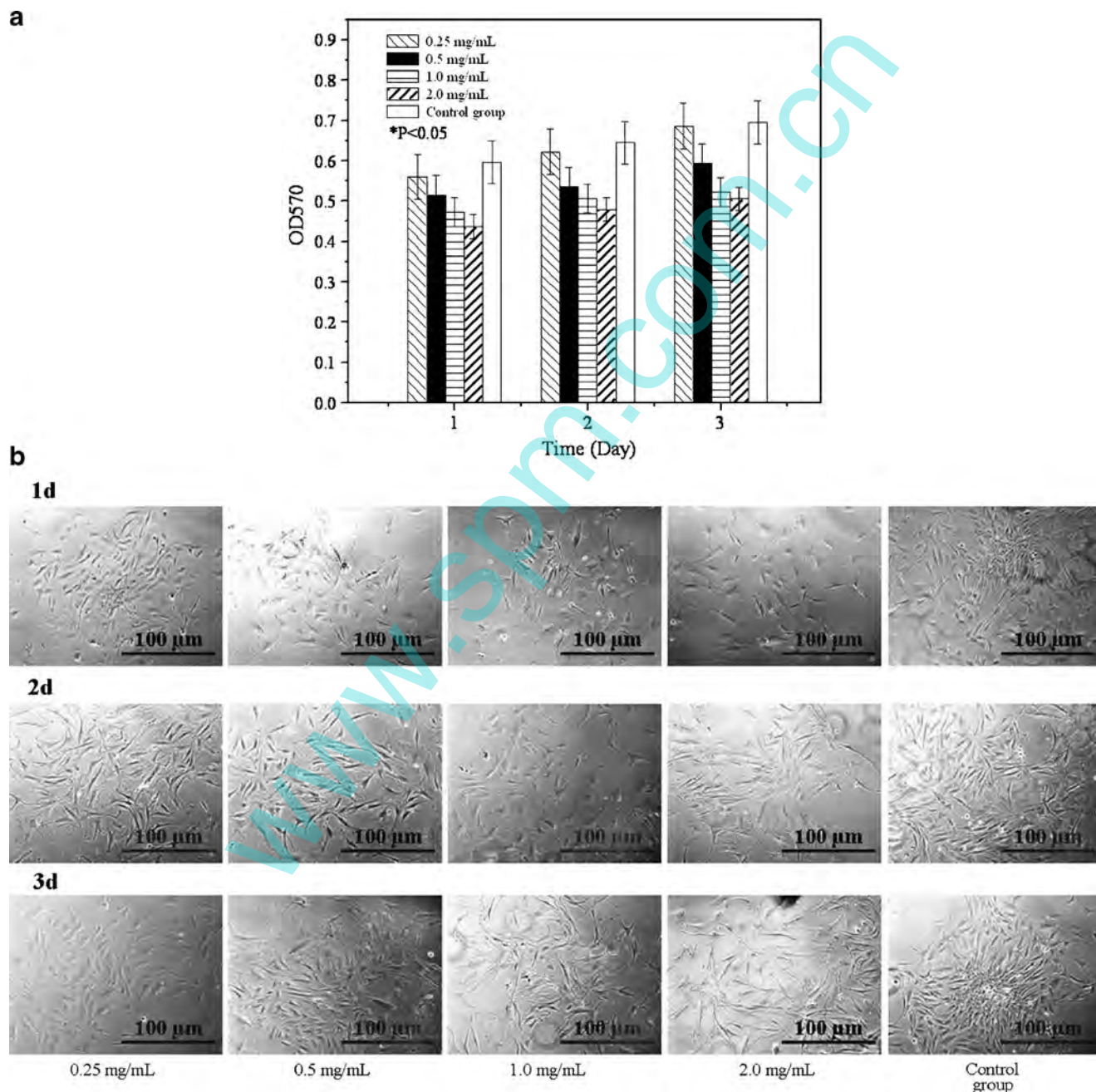


**Fig. 10** **a** MTT Assay **b** Optical microscopic observation of osteoblasts growth on the different concentration of the poly(PEG:CPP:SA) terpolymers micelles.

This shows that there was a certain percentage of cell death. The medication micelles are usually at low polymer concentration due to the dilution *in vivo*. Cell cytotoxicity study implied that the poly(PEG:CPP:SA) terpolymer micelles at low concentration were biocompatible. Thus, these micelles could be regarded as a safe drug delivery carrier.

DOX.HCl was selected as the therapeutic agent, and the loading, *in vitro* drug release and cytotoxicity of the nanocarriers were investigated in depth and compared against the behaviors of the host nanomaterial and the small molecule drug, each individually and together (54). The DOX.HCl loading efficiency was  $70 \pm 5\%$ , and the DOX loading content was 3.2%. Fig. 11(a) presents the *in*

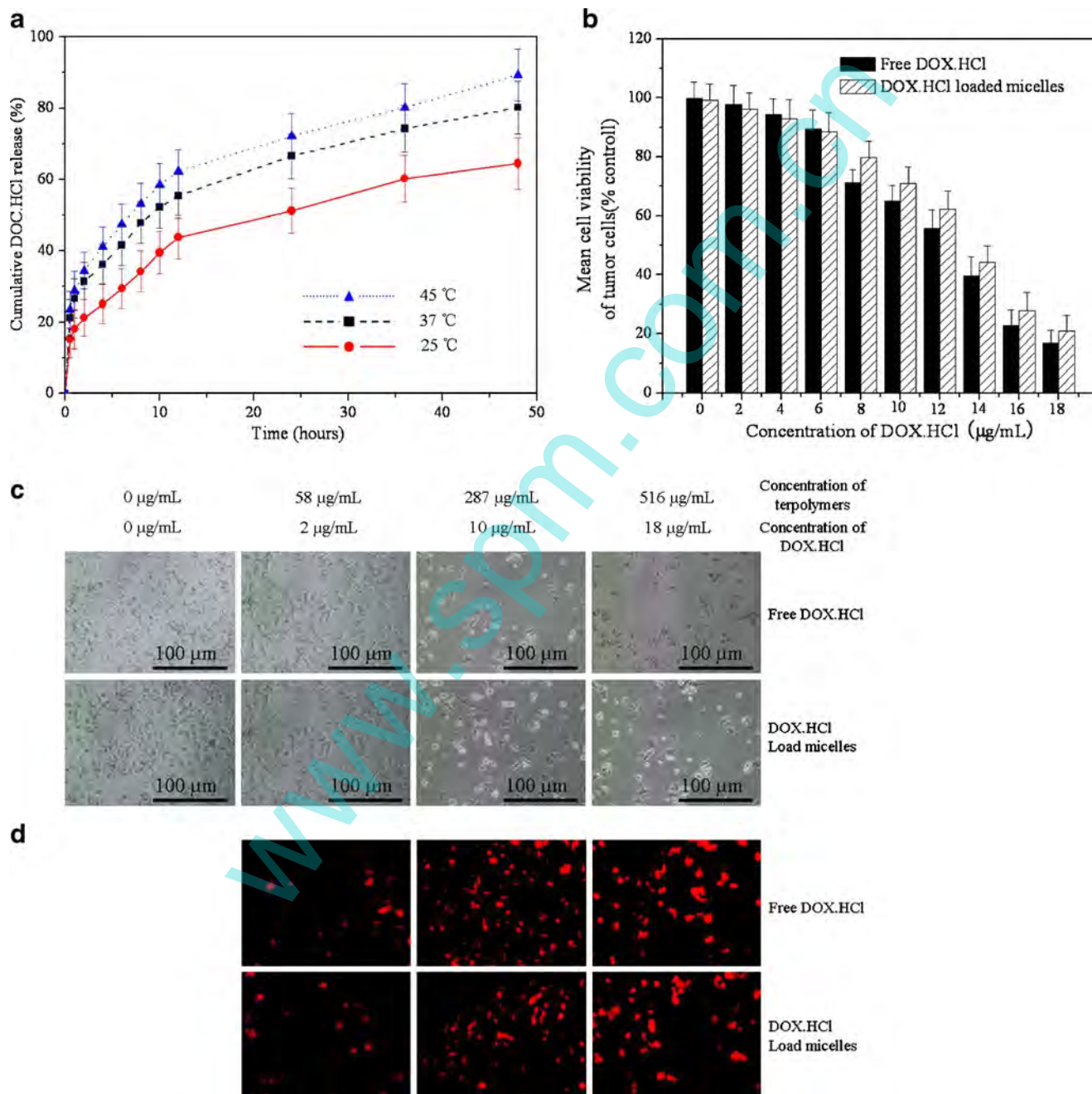


**Fig. 11** **a** *In vitro* drug release profiles of DOX.HCl-loaded micelles in PBS solution at pH 7.4 at 25°C, 37°C and 45°C, **b** *In vitro* tumor cell growth inhibition assay, **c** Optical microscopic observation and **d** Fluorescence microscopy study for the different concentrations of free DOX.HCl and the DOX.HCl-loaded poly(PEG:CPP:SA) (20:20:60) terpolymers micelles for 48 h.

*in vitro* release profiles of DOX.HCl-loaded micelles in phosphate-buffered saline (PBS) at pH 7.4. DOX.HCl-loaded micelles exhibited a relatively rapid burst release in the first stage followed by a sustained and slow release over a prolonged time up to 12 h, and release behavior remained constant after 48 h. Furthermore, the rate of DOX.HCl release at 45°C was about 1.5 times faster than that at 25°C. Based on this work, the drug release was accelerated dramatically on account of the thermo-induced structural change of the polymeric micelles. The polymeric micelles became hydrophobic above the LCST, leading to the deformation of micellar structure. As a result, the drug was released quickly from the micelles. In other words, the temperature change led to the deformation and precipitation of the core-shell micelles, thereby causing the enhanced release amount of the drug.

The MTT assay was performed to evaluate whether micelles influenced the cytotoxicity of DOX.HCl (Fig. 11). Both DOX.HCl-loaded terpolymer micelles and free DOX.HCl at various concentrations significantly influenced the growth of the HepG2 tumor cells at a certain dose. Fig. 11b displays the effect of drug concentration on cell viability of the HepG2 tumor cells. At the same drug concentration, cell viability of the tumor cells with free DOX.HCl is lower than that with DOX.HCl-loaded micelles, which indicates that the drug of the DOX.HCl-loaded micelles is released in an extended behavior. It is accorded with the release study, which showed that only 80% DOX.HCl released from these micelles within 48 h. As seen from Fig. 11c, the cell morphology and amount for the samples with 2.0 µg/mL DOX.HCl are similar to the control group, suggesting that the samples have good cell viabilities. In contrast, the cells became rounded, and the numbers of the cells reduced obviously as the drug concentration increased. As a greater amount of DOX.HCl could be intracellularly delivered into cells in the form of nano-sized micelles by endocytosis, the cells were more vulnerable to the cytotoxic effect of DOX.HCl (55). It shows that the influence of the DOX.HCl became more visible due to the increases of the drug concentration. The cell morphology of DOX.HCl-loaded micelles and free DOX.HCl were also studied by fluorescence microscopy. The red fluorescence from DOX.HCl was employed to study the cell morphology. As shown in Fig. 11d, the cells became rounded, and some amount of DOX.HCl-loaded micelles was swallowed by the tumor cells as the drug concentration increased. At this moment, the mechanism of cellular uptake of these micelles is not clear and remains to be further investigated. Compared with other existing polymeric systems (56,57), these DOX.HCl-loaded micelles were equally effective for suppressing the growth of the tumor cells.

## CONCLUSIONS

This study demonstrated that the amphiphilic poly(PEG:CPP:SA) terpolymers are a promising drug carrier. The micelles with low polydispersity of diameter and low CMC were formed from the terpolymers in an aqueous phase. Their assembly behaviors depended on the ratio of PEG/(CPP and SA) blocks, the terpolymers concentration and the environmental temperature. The CMC values of the terpolymers and the temperature of the sol-to-gel transition decreased with the increase of CPP and SA chains. The hydrodynamic diameters of the polymeric micelles increased as the degree of polymerization of the hydrophobic chains increased. The temperature of the aqueous phase also influenced the aggregate of the polymeric micelles. For poly(PEG:CPP:SA) (20:20:60), the spherical micelles could be observed by AFM and TEM at the concentration of 4.0 mg/mL, and when the concentration was raised to 10 wt%, the gel formed at 34°C. Moreover, the sol-nanogel transition could be achieved at body temperature, and the transition was almost irreversible with decreasing temperature, which is very important for applications in nanomedicine. The DOX.HCl-loaded micelles could be well-dispersed in water and could keep stable for a long time. The *in vitro* release profiles at different temperatures consist of a burst release followed a sustained release. Cell cytotoxicity results indicated that the terpolymers were of excellent biocompatibility, and the DOX.HCl-loaded micelles were effective to inhibit the growth of tumor cells.

## ACKNOWLEDGEMENTS

This work was partially supported by National Natural Science Foundation of China (30970723), Programs for New Century Excellent Talents in university, Ministry of Education of China (NCET-07-0719) and Sichuan Prominent Young Talent Program (08ZQ026-040).

## REFERENCES

1. Basarkar A, Singh J. Poly (lactide-co-glycolide)-polymethacrylate micelles for intramuscular delivery of plasmid encoding interleukin-10 to prevent autoimmune diabetes in mice. *Pharm Res.* 2009;26:72–81.
2. Allen TM, Cullis PR. Drug delivery systems: entering the main stream. *Science* 2004;303:1818–22.
3. Hu XL, Liu S, Chen XS. Biodegradable amphiphilic block copolymers bearing protected hydroxyl groups: synthesis and characterization. *Biomacromolecules* 2008;9:553–60.
4. Kataoka K, Kwon GS, Yokoyama M, Okano T, Sakurai Y. Block copolymer micelles as vehicles for drug delivery. *J Control Release.* 2006;24:119–32.
5. Branco MC, Schneider JP. Review: Self-assembling materials for therapeutic delivery. *Acta Biomaterialia.* 2009;5:817–31.

6. Cai SS, Vijayan KS, Cheng D, Lima EM, Discher DE. Micelles of different morphologies—advantages of worm-like filomicelles of PEO-PCL in paclitaxel delivery. *Pharm Res*. 2007;24:2099–109.
7. Martini L, Attwood D, Collett J. The bioadhesive properties of a triblock copolymer of  $\epsilon$ -caprolactone and ethylene oxide. *Int J Pharm*. 2005;113:223–9.
8. Cohn D, Salomon AH. Biodegradable multiblock PEO/PLA thermoplastic elastomers: molecular design and properties. *Polymer* 2005;46:2068–75.
9. Lavasanifar A, Samue J, Kwon GS. Poly(ethylene oxide)-block-poly(L-amino acid) micelles for drug delivery. *Adv Drug Deliv Rev*. 2005;54:169–90.
10. Rapoport N. Combined cancer therapy by micellar-encapsulated drug and ultrasound, nanotechnology for cancer therapy. *Boca Raton*. 2006;2:417–37.
11. Vakil R, Kwo GS. Poly(ethyleneglycol)-b-poly( $\epsilon$ -caprolactone) and PEG-phospholipid form stable mixed micelles in aqueous media. *Langmuir* 2006;22:9723–9.
12. Jeong B, Bae YH, Kim SW. Thermoreversible gelation of PEG-PLGA-PEG triblock copolymer aqueous solutions. *Macromolecules* 2001;32:7064–9.
13. Joo MK, Sohn YS, Jeong B. Stereoisomeric effect on reverse thermal gelation of poly(ethylene glycol)/poly(lactide) multiblock copolymer. *Macromolecules* 2007;40:5111–5.
14. Yang L, Xian ZZ, Wei J, Suming L. Micelles formed by self-assembly of poly(lactide)/poly(ethylene glycol) block copolymers in aqueous solutions. *J Colloid Interface Sci*. 2007;31:4470–7.
15. Wang YP, Xu HP, Zhang X. Tuning the amphiphilicity of building blocks: controlled self-assembly and disassembly for functional supramolecular materials. *Adv Mater*. 2009;21:2849–64.
16. Bae Y, Fukushima S, Harada A, Kataoka K. Design of environment-sensitive upramolecular assemblies for intra cellular drug delivery: polymeric micelles that are responsive to intracellular pH change. *Angew Chem Int Ed Engl*. 2003;42:4640–3.
17. Webber GB, Wanless EJ, Armes SP, Tang YQ, Li YT, Biggs S. Nano-anemones: stimulus-responsive copolymer-micelle surfaces. *Adv Mater*. 2004;16:1794–8.
18. Dong Y, Feng SS. Methoxypoly (ethyleneglycol)-poly(lactide) (MPEG-PLA) nanoparticles for controlled delivery of anticancer drugs. *Biomaterials* 2004;25:2843–9.
19. Chen G, Hoffman AS. Graft copolymers that exhibit temperature-induced phase transitions over a wide range of pH. *Nature* 1995;373:49(R)–52.
20. Liu TY, Hu SH, Liu DM, Chen SY, Chen IW. Review: biomedical nanoparticle carriers with combined thermal and magnetic responses. *Nano Today*. 2009;4:52–65.
21. Hoffman AS. Applications of thermally reversible polymers and hydrogels in therapeutics and diagnostics. *J Control Release*. 1987;6:297–305.
22. Peppas NA, Bures P. Hydrogels in pharmaceutical formulations. *Eur J Pharm Biopharm*. 2005;50:27–46.
23. Hoffman AS. Hydrogels for biomedical applications. *Adv Drug Deliv Rev*. 2002;43:3–12.
24. Farhood N, Mohammad N. Biodegradable micelles/polymerosomes from fumaric/sebacic acids and poly(ethylene glycol). *Biomaterials* 2006;24:1175–82.
25. Cohn D, Lando G, Sosnik A, Garty S, Levi A. PEO-PPO-PEO based poly(ether ester urethane)s as degradable thermo-responsive multiblock copolymers. *Biomaterials* 2006;27:1718–27.
26. Jeong B, Bae YH, Lee DS, Kim SW. Biodegradable block copolymers as injectable drug-delivery systems. *Nature* 1997;388:860–2.
27. Zana R, Binanlimb W, Kamenka N. Ethyl(hydroxyethyl) cellulose cationic surfactant interactions-electrical conductivity, self-diffusion, and time-resolved fluorescence, quenching investigations. *J Phys Chem*. 2007;96:5461–5.
28. Kamenka N, Burgaud L, Zana R. Electrical conductivity, self-diffusion, and fluorescence probe investigations of the interaction between sodium dodecyl-sulfate and ethyl(hydroxyethyl) cellulose. *J Phys Chem*. 2004;98:6785–9.
29. Kim IS, Lee SK, Park YM, Lee YB, Shin SC, Lee KC *et al*. Physicochemical characterization of poly(L-lactic acid) and poly(D, L-lactide-co-glycolide) nanoparticles with polyethylenimine as gene delivery carrier. *Int J Pharm*. 2005;298:255–62.
30. Karnik R, Gu F, Basto P. Microfluidic platform for controlled synthesis of polymeric nanoparticles. *Nano Lett*. 2008;8:2906–12.
31. Kataoka K, Harada A, Nagasaki Y. Block copolymer micelles for drug delivery: design, characterization and biological significance. *Adv Drug Deliv Rev*. 2004;47:113–31.
32. Fiegel J, Fu J, Hanes J. Synthesis and characterization of PEG-based ether-anhydride terpolymers: novel polymers for controlled drug delivery. *Macromolecules* 2004;37:7174–80.
33. Zhang N, Guo SR. Synthesis and micellization of amphiphilic poly(sebacic anhydride)-poly(ethylene glycol)-poly(sebacic anhydride) block copolymers. *J Polym Sci Part: A*. 2006;44:1271–8.
34. Lee JS, Joo MK, Oh HJ. Injectable gel: poly(ethylene glycol)-sebacic acid polyester. *Polymer* 2006;47:3760–6.
35. Rosen HB, Chang J, Wnek GE, Linhardt RJ, Langer R. Bioerodible polyanhydrides for controlled drug delivery. *Biomaterials* 1983;4:131–3.
36. Zhao C, Wang Y, Winnik MA, Riess G, Croucher MD. Fluorescence probe technique used to study micelle formation in water-soluble block co-polymer. *Langmuir* 1999;6:514–6.
37. Forrester M, Won CY, Malick A, Kwon G. *In vitro* release of poly(ethylene glycol)-b-poly( $\epsilon$ -caprolactone) micelle. *J Control Release*. 2006;110:370–7.
38. Fiegel J, Fu J, Hanes J. Poly(ether-anhydride) dry powder aerosols for sustained drug delivery in the lungs. *J Control Release*. 2004;96:411–23.
39. Liu Y, Zhao ZX, Wei J. Micelles formed by self-assembly of polylactide/poly(ethylene glycol) block copolymers in aqueous solutions. *J Colloid Interface Sci*. 2007;314:470–7.
40. Adams M, Lavasanifar A, Kwon G. Amphiphilic block copolymers for drug delivery. *J Pharm Sci*. 2005;92:1343–55.
41. Kabanov A, Alakhov V. Pluronic block copolymers in drug delivery: from micellar nanocontainers to biological response modifiers. *Crit Rev Ther Drug*. 2007;19:1–72.
42. Zhang L, Eisenberg A. Multiple morphologies of crew-cut aggregates of polystyrene-b-poly(acrylic acid) block copolymers. *Science* 1995;268:1728–31.
43. Cabra H, Nakanishi M, Kumagai M, Jang WD, Nishiyama N, Kataoka K. A photo-activated targeting chemotherapy using glutathione sensitive camptothecin-loaded polymeric micelles. *Pharm Res*. 2007;24:2099–109.
44. Rapoport N. Physical stimuli-responsive polymeric micelles for anti-cancer drug delivery. *Prog Polym Sci*. 2007;32:962–90.
45. Oh KT, Bronich TK, Kabanov AV. Micellar formulations for drug delivery based on mixtures of hydrophobic and hydrophilic Pluronic block copolymers. *J Control Release*. 2004;94:411–22.
46. Zhe J, Sun X, Moon H, Soo Y. Thermosensitive micelles from PEGylated oligopeptides. *Polymer* 2007;48:3673–8.
47. Yan H, Yong HY, Zhou F. Synthesis and supramolecular self-assembly of thermosensitive amphiphilic star copolymers based on a hyperbranched polyether, core. *J Polym Sci Part: A*. 2008;46:668–81.
48. Fraylich F, Wang WX, Sheff KS, Alexander C, Saunders B. Poly(D,L-lactide-co-glycolide) dispersions containing pluronics: from particle preparation to temperature-triggered aggregation. *Langmuir* 2008;24:7761–8.
49. Tang Y, Singh J. Biodegradable and biocompatible thermosensitive polymer based injectable implant for controlled release of protein. *Int J Pharm*. 2009;365:34–43.



50. Gong Y, Shi S, Wu L, Gou ML, Yin QQ, Guo QF *et al.* Biodegradable *in situ* gel-forming controlled drug delivery system-based on thermosensitive PCL-PEG-PCL hydrogel. Part 2: sol-gel-sol transition and drug delivery behavior. *Acta Biomater.* 2009;5:3358-70.
51. Nagahama KJ, Imai YC, Nakayama T, Ohmura J, Ouchi T, Ohya Y. Thermo-sensitive sol-gel transition of poly(depsipeptide-co-lactide)-g-PEG copolymers in aqueous solution. *Polymer* 2009;23:1-9.
52. Yu L, Chang GT, Zhang H, Ding JD. Temperature-induced spontaneous sol-gel transitions of poly(D,L-lactic acid-co-glycolic acid)-b-poly(ethylene glycol)-b-poly(D,L-lactic acid-co-glycolic acid) triblock copolymers and their end-capped derivatives in water. *J Polym Sci Part: A.* 2007;45:1122-33.
53. Mata JP, Majhi PR, Guo C, Liu HZ, Bahadur P. Concentration, temperature, and salt-induced micellization of a triblock copolymer Pluronic L64 in aqueous media. *J Colloid Interface Sci.* 2005;292:548-56.
54. Packhaeuser CB, Schnieders J, Oster CG, Kissel T. *In situ* forming parenteral drug delivery systems: an overview. *Euro J Pharm Biopharm.* 2004;58:445-55.
55. Lasic DD. Doxorubicin in sterically stabilized liposomes. *Nature* 1996;380:561-2.
56. Lee ES, Na K, Bae YH. Doxorubicin loaded pH-sensitive polymeric micelles for reversal of resistant MCF-7 tumor. *J Control Release.* 2005;103:405-18.
57. Yoo HS, Park TG. Folate receptor targeted biodegradable polymeric doxorubicin micelles. *J Control Release.* 2004;96:273-83.

www.spm.com.cn